Surface coating on carbon nanofibers with alumina precursor by different synthesis routes

A. Borrell[1]*, V.G. Rocha[2], R. Torrecillas[1], A. Fernández[2]

[1]*Centro de Investigación en Nanomateriales y Nanotecnología (CINN) (Consejo Superior de Investigaciones Científicas - Universidad de Oviedo - Principado de Asturias), Parque Tecnológico de Asturias, 33428 Llanera (Asturias), Spain*

[2]*Fundación ITMA, Parque Tecnológico de Asturias, 33428 Llanera (Asturias), Spain*

*Corresponding author. Address: *Centro de Investigación en Nanomateriales y Nanotecnología (CINN), Parque Tecnológico de Asturias, 33428 Llanera (Asturias), Spain*. Tel.: +34 985 980 058; fax: +34 985 265 574. E-mail address: a.borrell@cinn.es (A.Borrell).

ABSTRACT

Alumina-reinforced carbon nanofiber nanocomposites were prepared using different routes; powders mixture, colloidal route and sol-gel process followed by spark plasma sintering (SPS). CNFs/xAl_2O_3 (x=10-50 vol.%) were prepared through nanopowders mixing in a high-energy attrition milling. The main limitations in the preparation of this kind of nanocomposites are related to the difficulty in obtaining materials with a homogeneous distribution of both phases and the different chemical nature of CNFs and Al_2O_3, which causes poor interaction between them. A surface coating of CNFs by wet chemical routes with an alumina precursor is proposed as a very effective way to improve the interaction between CNFs and Al_2O_3. An improvement of 50% in fracture strength was found for similar nanocomposite compositions when the surface coating

1

was used. The improved mechanical properties of these nanocomposites are caused by stronger interaction between the CNFs and Al_2O_3.

1. INTRODUCTION

The development of new alumina-reinforced carbon nanofiber composite materials with excellent mechanical and electrical properties is useful for a wide range of industrial applications. Thanks to their exceptional mechanical, electrical and thermal properties, carbon nanofibers (CNFs) encourage the development of advanced materials through their incorporation in matrices such as polymers [1-2], metals [3-4] and ceramics [5-6]. Recently, there have been major developments in polymer matrix composites reinforced by CNFs, where properties achieved have been clearly higher than those corresponding to pure polymeric material. Nevertheless, there have been few advances for CNFs composites in ceramic and metal matrix, because getting good dispersion of CNFs in these systems is technically challenging [7-10]. Alumina is a ceramic commonly used in the development of advanced ceramics [11], especially in functional applications because of its relatively high hardness, good oxidation resistance and chemical inertness. There are studies [12-14] showing that the addition of CNFs to alumina matrix does not produce a reinforcement in the materials obtained. This has been attributed to an inhomogeneous dispersion of CNFs in the composite materials due to the formation of CNFs aggregates as a consequence of strong Van der Waals interactions [15-16], which sometimes cause anisotropy in the final properties of the materials. In the majority of the previous studies, alumina powders are mechanically

mixed with CNFs in order to prepare CNFs/alumina composites that have, in some cases, properties lower than expected. Generally, the addition of carbon nanofibers as reinforcement leads to slight improvements in the fracture strength although the hardness and/or toughness are degraded [7]. These results are related to the formation of CNFs agglomerates and the weak CNFs/Al_2O_3 interface. A promising solution for avoiding these problems could be the direct synthesis of alumina nanoparticles on the CNFs surface. There are many processes for synthesizing ceramic nanopowders such as mechanical synthesis, vapor phase reaction, precipitation and combustion or sol-gel methods [17]. Although there are different limitations in all the aforementioned methods [18-19], wet chemical methods are especially useful for this purpose. In many cases conventional processing methods for traditional powder mixture are relieved by chemical synthesis methods that allow the reactions, nucleation and growth of nanocrystals at molecular level to be controlled.

In order to obtain CNFs/alumina dense materials, spark plasma sintering (SPS) was used as the sintering technique. This is also known as field assisted sintering technique (FAST) and it is a new sintering technique that can consolidate powder compacts by applying an on-off dc electric pulse under uniaxial pressure [20]. This technique can work at heating rates of hundreds degrees per minute, reaching high temperatures in a short time, and producing dense materials [21]. These features allow the achievement of microstructures unattainable by other sintering techniques.

The aim of this work was to develop alumina-reinforced carbon nanofiber nanocomposites. In order to improve the affinity between the components, the surface coating of CNFs with an alumina nanoparticles precursor was studied by the sol-gel and colloidal processes. The "surface coating" composites have been evaluated in comparison with materials prepared by conventional powders mixing. The materials

obtained were compared in terms of their microstructural evolution, mechanical and electrical properties.

2. EXPERIMENTAL PROCEDURE

2.1. Preparation of composite powders

2.1.1. Mixed powders

The materials used in this study were commercial carbon nanofibers (CNFs) having an average outer diameter of 20-80 nm and lengths >30 μm, supplied by Group Antolin Engineering, (Spain). These CNFs were generated via vapor phase growth (VGCNFs) [22] using a floating catalyst of nickel in solution (6-8%). α-Al_2O_3 nanopowder (Taimei TM-DAR Chemicals Co. Ltd, Japan) with an average particle size of 153 nm and a purity of 99.99% was used as a second phase. The powder mixtures, CNFs/Al_2O_3 = 90/10 - 80/20 - 70/30 – 60/40 – 50/50 vol.%, were dispersed in ethanol (Panreac Quimica) with a high-energy attrition milling (Union Process, EE.UU) using alumina media of 2 mm diameter at 400 rpm and milling times of 1 hour. After milling, the resulting slurry was dried at 60 ºC and the dried powder was sieved under 60 μm.

2.1.2. Surface coating of CNFs

The surface coating of CNFs was carried out employing two different processing routes, colloidal and sol-gel. Aluminum chloride hexahydrate, $AlCl_3 \cdot 6H_2O$ (>99% purity, Fluka), was used as the alumina precursor in both cases. The alumina precursor was added to a CNFs water dispersion eventually yielding composites with a 10 vol.% Al_2O_3. In the colloidal synthesis route or heterogeneous precipitation method [23], CNFs were dispersed in distilled water using magnetic stirring. The appropriate amount of aluminum chloride, also dissolved in distilled water, was added dropwise to the water

4

dispersion of CNFs. The slurry was first dried maintaining magnetic stirring at 60-70 ℃ and subsequently at 120 ℃ in order to eliminate wastewater. In the case of the sol-gel method, the aluminum chloride was dissolved in distilled water under stirring and, in order to control the chemical reactivity in the solution, the pH was adjusted with ammonium hydroxide solution (Fluka, 28% in water), keeping a constant pH value (~9) throughout the process in order to control the sol formation. Subsequently, CNFs were added to the aluminum chloride solution and mixed thoroughly by stirring. Finally, the solution was heated gently to form a gel. After aging for 24 h, a gelatinous product was obtained. The resultant amorphous gel was dried at 60-70 ℃ and subsequently at 120 ℃ for 24 h in order to eliminate wastewater. The CNFs/Al_2O_3 powders were ground by mortar and pestle, and sieved below 60 μm to achieve a uniform distribution of particle sizes. Thermogravimetric analysis of the modified powders (TGA Star System, Mettler Toledo) were carried out up to 1000 ℃, using a 5 ℃ min^{-1} heating rate under an argon atmosphere in order to check the temperature to remove solvent and chloride wastes.

2.2. SPS and characterization of sintered bodies

The powder samples were placed into a graphite die with an inner diameter of 20 mm and cold uniaxially pressed at 30 MPa. Then, they were introduced in a spark plasma sintering apparatus HP D 25/1 (FCT Systeme GmbH, Rauenstein, Germany) under low vacuum (10^{-1} mbar) and sintered at 1500 ℃ for 1 min under an applied pressure of 80 MPa and a heating rate of 100 ℃ min^{-1}. Bulk density of the sintered bodies was measured by the geometric method from weight and geometric volume of the material. Relative densities were calculated as the relation between geometrical and theoretical densities. The fracture strength was measured using biaxial testing employing the equations of Kirstein and Woolley [24], Vitman and Pukh [25], and the standard

specification ASTM F394-78 [26]. All tests were performed at room temperature using the universal machine Instron (Model 8562) with a cross-head displacement speed of 0.002 mm s^{-1}. The samples for hardness analysis were previously polished (Struers, model RotoPol-31) with diamond to 1 μm roughness. The hardness of the materials was determined using the indentation technique (Buehler, model Micromet 5103) with a conventional diamond pyramid indenter. The diagonals of each indentation were measured using an optical microscope. Measuring conditions for the Vickers hardness, H_v, were an applying load of 2 N for 10 s and the standard specification ASTM E92-72. The value of H_v is the relationship between applied load P and the surface area of the diagonals of indentation [27]. X-ray diffraction (XRD) analysis was performed on a Siemens X-ray diffractometer (Model D 5000), using "Bragg-Brentano" geometry with Cu-k$_\alpha$ radiation (λ=0.15418 nm, 40 kV, 30 mA). The measurements were performed in the range of 15-80º with a step size and time of reading of 0.02º and 0.3 s, respectively. Fracture surfaces of sintered samples were characterized by scanning electron microscopy (SEM, Zeiss DSM 950). The electrical resistivity of monolithic and composite materials was determined according to ASTM C611. The specimens were placed between two sheets of copper connected to a power supply, which allowed working at different current intensities. The measures were carried out by fixing the intensity of the current at 0.5 A using a multimeter of fixed pegs (9.55 mm separation), determining the voltage drop.

3. RESULTS AND DISCUSSION

3.1. Composites obtained from mixing powders

Table 1 summarizes the main properties such as density, hardness and fracture strength of the different CNFs/Al$_2$O$_3$ composites prepared by powder mixing and sintered by

SPS at 1500 ºC. Relative densities slightly increase with alumina addition from 10-40 vol.% Al_2O_3 being always around 90%. However, when 50 vol.% Al_2O_3 is added the relative density reached ~96%. This indicates that alumina powder addition helps the sinterability of CNFs and this effect is not proportional to ceramic phase content. The density improvement of the nanocomposites can only be observed for alumina contents of 40-50 vol.%. This fact may be due to the activation of sintering mechanisms of the ceramic phase, a high alumina content being necessary.

In good correlation with the densities values it can be seen that the fracture strength only increases when alumina content in the composite is 50 vol.%. Fracture strength of CNFs+50 vol.% Al_2O_3 composite is 134 MPa, and this value is twice as much as corresponding to 40 vol.% Al_2O_3 composite. So, when alumina content is equal or greater than 50 vol.% Al_2O_3, it can be considered that the alumina behaves as the matrix. Therefore, for a relatively low volume fraction of alumina, the fracture strength of the nanocomposite is similar to that of a carbon material, approximately 60 MPa [10], and a similar behavior to ceramic material is observed only when the alumina content is high. However, the hardness of the composites increases gradually with the ceramic phase addition. The reason for the different trend in both mechanical properties with alumina content is related to the influence of second phase nanoparticles on matrix behavior. In the case of hardness, the presence of alumina nanoparticles, characterized by its high hardness, leads to local reinforcement and this effect depends on nanoparticles content. However, the material fracture strength is proportional to its fracture toughness and therefore, to its opposition to crack propagation. Only when the matrix behavior changes as in the case of high alumina content, is a major improvement in material fracture strength observed.

In order to study this effect, Figure 1 shows SEM fracture surfaces micrographs of CNFs/Al_2O_3 composites sintered by SPS at 1500 ºC with 10 (a), 40 (b) and 50 (c) vol.% Al_2O_3. Due to the nature, content, size and shape of the CNFs present in these composites, the components identification by SEM is very difficult, and the ceramic phase is not well identified until the alumina content in the composite is around 50 vol.% Al_2O_3 (Fig. 1c). However, in micrographs corresponding to composites with lower ceramic content, alumina nanoparticles were identified by a circle (Fig 1a). It is important to note the small size of those nanoparticles. Taking into account the starting grain size of the alumina particles (~150 nm) it can be seen that after sintering at 1500 ºC the final size is very similar. This shows that the grain growth of the ceramic component in the nanocomposites is suppressed by CNFs presence. As was previously explained, the fracture mode of the material with a 50 vol.% of Al_2O_3 is predominantly intergranular, and is reminiscent of the behavior of a ceramic material (Fig. 1c). Therefore, this micrograph suggests the matrix change, when the alumina volume content achieves a 50 vol.%.

The electrical resistivity of all CNFs/Al_2O_3 composite materials, measured at room temperature was ~10^{-2} Ω cm. This value corresponded to the carbon nanofibers raw material. This result shows that whereas the conductive component content, in this case the carbon nanofibers, is over the critical percolation volume fraction [28], the electrical conductivity of the nanocomposites remains constant. So, very useful properties have arisen in the CNFs+50vol.% Al_2O_3 composite. It has the same electrical conductivity but with a considerably higher fracture strength (134 vs. 60 MPa) than those obtained in 100% CNFs material [10]. This new composite will be especially useful because it could replace graphite materials [29] in applications in which their uses are now forbidden due to their low mechanical properties. The homogeneous distribution of

8

ceramic and carbon components in the nanocomposite allows the obtaining of a material that combines good electrical and mechanical properties.

3.2. Composites obtained from colloidal and sol-gel methods

Another problem in obtaining ceramic-carbon composites is related to their different surface properties, reflected in a weak interface [30]. So, in order to explore the possibility of improving this feature, the preparation of these nanocomposites by two wet chemical synthesis routes was studied.

Figure 2 shows the thermogravimetric analysis corresponding to the powders synthesized by colloidal and sol-gel methods: the curve of sol-gel powders shows two weight loss steps. In the first step (160-360 ºC) there is a weight loss of ~32 wt.% with T_{max} at 285 ºC. This is due to the residual solvent adsorbed in the powders caused by a three-dimensional network formed in the sol-gel process that retains more water. In the second step (360-680 ºC) there is a weight loss of 8 wt.%. This loss tendency can be associated with the chloride elimination. Finally, at temperatures higher than 720 ºC the weight loss stabilizes.

Table 2 shows the two weight loss steps of the colloidal composite powder. T_{max} takes place at 225 ºC and the first step weight loss ~12 wt.%, is considerably lower than the sol-gel process due to the easier elimination of water in this material during the drying steps. The second weight loss step takes place between 360-680 ºC and the weight loss is very similar to the sol-gel powder ~10 wt.% that could be expected considering that it is related to the chloride removal and the aluminum chloride amount used in both cases was the same. Taking into account these results, the powders were thermally treated at 700 ºC for 2 h in an argon atmosphere, in order to remove precursor wastes without affecting the carbon nanofibers.

Figure 3 shows the XRD-patterns of sintered bodies. Both composite powders led to α-alumina and graphite after sintering up to 1500 ºC by SPS. The lower relative intensity and wider peaks of alumina in the composite obtained from sol-gel powder, compared with material prepared by the colloidal route is indicative of a smaller crystal size, as they have the same content in ceramic phase.

Table 3 summarizes the properties such as the density, hardness and fracture strength of the different CNFs+10vol.% Al_2O_3 composites sintered by SPS at 1500 ºC. The surface coating by colloidal or sol-gel method should improve the mechanical properties as it could be predicted from their relative densities. In both cases the relative density of composites (~93%) are slightly higher than that achieved in the material with similar composition obtained by powder mixing (~90%). The sol-gel process allows the formation of a three dimensional network which perfectly interconnects the particles in the whole volume. Consequently, carbon nanofibers which have been previously well dispersed in the solvent will be homogeneously coated by the gel layer. Heat treatment will lead to the formation of alumina nanoparticles that are very well dispersed in the composite. Although the colloidal route process seems to be very similar to the sol-gel process the differences are very significant. In the colloidal route, carbon nanofibers are preferential nucleation sites for the alumina precursor and this mechanism is known as heterogeneous precipitation. However, another process is in competition with heterogeneous precipitation, the nucleation and growth of aluminum hydroxide particles directly from the solution, this being homogeneous precipitation.

The alumina nanoparticles formed by heterogeneous precipitation would be similar to those obtained by the sol-gel method. However, particles formed by homogeneous precipitation are not linked to the carbon nanofibers surface and so i) they can grow, achieving greater size and leading to potential defects and ii) they are not contributing to

ceramic-carbon interface reinforcement. In fact, the fracture strength of the sintered body of the sol-gel composite powder is almost 50% higher than that obtained by the mixed powders composite and considerably higher than colloidal processing route composite.

As could be expected, the electrical resistivity of both composites, obtained by colloidal and sol-gel methods is 10^{-2} Ω cm, this value being similar to the material obtained by mixing powders. Additionally, the electrical resistivity was measured in both directions, parallel and perpendicular to the direction of the applied pressure during sintering, and in both directions the same results were achieved. This is indicative of a homogenous dispersion of CNFs and alumina.

4. CONCLUSIONS

The addition of Al_2O_3 powders as a second phase to the CNFs matrix improves the densification of materials based on CNFs. High alumina contents are necessary to improve mechanical properties of CNFs/alumina nanocomposites by powder mixture, while the surface coating of carbon nanofibers using a precursor of alumina leads to an improved composite even with only a 10 vol.% Al_2O_3. All composites show an electrical conductivity similar to the raw carbon nanofibers, therefore alumina could be used as reinforcement phase of carbon composites. The surface coating of carbon nanofibers using a precursor of alumina is a very useful method for obtaining CNFs/Al_2O_3 composites, due to an improvement of interface between the CNFs and alumina. A major improvement in the mechanical properties of CNFs/Al_2O_3 nanocomposites was achieved by sol-gel CNFs surface coating with an alumina precursor. This nanocomposite shows almost a 50% higher fracture strength compared to composites prepared by conventional mixing powders.

References

[1] Ma H, Zeng J, Realff ML, Kumar S, Schiraldi DA. Structure, properties, and processing of polyester/nano carbon composite fibers. Compos Sci Technol 2003;63:1617–28.

[2] Higgins BA, Brittain WJ. Polycarbonate carbon nanofiber composites. Eur Polym J 2005;41:889–93.

[3] Kim IS, Lee SK. Fabrication of carbon nanofiber/Cu composite powder by electroless plating and microstructural evolution during thermal exposure. Scripta Mater 2005;52:1045–49.

[4] Hammel E, Tang X, Trampert M, Schmitt T, Mauthner K, Eder A, Pötschke P. Carbon nanofibers for composite applications. Carbon 2004;42:1153–58.

[5] Matsui K, Lanticse LJ, Tanabe Y, Yasuda E, Endo M. Stress graphitization of C/C composite reinforced by carbon nanofibers. Carbon 2005;43:1577–79.

[6] Seghi S, Lee J, Economy J. High density carbon fiber/boron nitride matrix composites: Fabrication of composites with exceptional wear resistance. Carbon 2005;43:2035–43.

[7] Hirota K, Takaura Y, Kato M, Miyamoto Y. Fabrication of carbon nanofibers (CNF)-dispersed Al_2O_3 composites by pulsed electric-current pressure sintering and their mechanical and electrical properties. J Mater Sci 2007;42:4792–4800.

[8] Maensiri S, Laokul P, Klinkaewnarong J, Amornkitbamrung V. Carbon nanofiber-reinforced alumina nanocomposites: Fabrication and mechanical properties. Mater Sci Eng A 2007;447:44–50.

[9] Duszová A, Dusza J, Tomásek K, Morgiel J, Blugand G, Kueblerd J. Zirconia/carbon nanofiber composite. Scripta Mater 2008;58:520–3.

[10] Borrell A, Fernandez A, Merino C, Torrecillas R. High density carbon materials obtained at relatively low temperature by spark plasma sintering of carbon nanofibers. Int J Mater Res 2010;101:112–8.

[11] Cranmer C. Overview of technical, engineering and advanced ceramics. Engineered Materials Handbook, Ceramic and Glasses. ASM International 1991;4.

[12] An JW, You DH, Lim DS. Tribological properties of hot-pressed alumina–CNT composites. Wear 2003;255:677–81.

[13] Siegel RW, Chang SK, Ash BJ, Stone J, Ajayan PM, Doremus RW, Schadler LS. Mechanical behavior of polymer and ceramic matrix nanocomposites. Scripta Mater 2001;44:2061–65.

[14] Laurent Ch, Peigney A, Dumortier O, Rousset A. Carbon nanotubes–Fe–Alumina nanocomposites. Part II: microstructure and mechanical properties of the hot-Pressed composites. J Eur Ceram Soc 1998;18:2005–11.

[15] Jiang L, Gao L, Sun J. Production of aqueous colloidal dispersions of carbon nanotubes. J Colloid Interface Sci 2003;260:89–94.

[16] Sun J, Gao L. Development of a dispersion process for carbon nanotubes in ceramic matrix by heterocoagulation. Carbon 2003;41:1063–68.

[17] Hida M, Yajima Y, Yamaguchi T, Taruta S, Kitajima K. Pulse electric current sintering of transition alumina/zirconia composite powders prepared by a novel sol-gel route. J Ceram Soc Jpn 2005;113:543–49.

[18] Shojaie-Bahaabad M, Taheri-Nassaj E. Economical synthesis of nano alumina powder using an aqueous sol–gel method. Mater Lett 2008;62:3364–6.

[19] Panchula ML, Ying JY. Mechanical synthesis of nanocrystalline α-Al$_2$O$_3$ seeds for enhanced transformation kinetics. Nanostruct Mater 1997;9:161–64.

[20] Joanna RG, Antonios Z. Sintering activation by external electrical field. Mater Sci Eng A 2000;287:171–77.

[21] Wang Y, Fu Z. Study of temperature field in spark plasma sintering. Mater Sci Eng B 2002;90:34–7.

[22] Ci L, Wei J, Wei B, Liang J, Xu C, Wu D. Carbon nanofibers and single-walled carbon nanotubes prepared by the floating catalyst method. Carbon 2001;39:329–35.

[23] Schehl M, Díaz LA, Torrecillas R. Alumina nanocomposites from powder alkoxide mixtures. Acta Mater 2002;50:1125–39.

[24] Kirstein AF, Woolley RM. Symmetrical bending of thin circular elastic plates on equally spaced point supports. J Res Nat Bur Stand C 1967;71:1–10.

[25] Vitman FF, Pukh VP. A method for determining the strength of sheet glass. Zavod Lab 1963;29:863–67.

[26] ASTM Standard F394-78, STM Annual Book of Standards, Vol. 15.02, Section 16. American Society for Testing and Materials, Philadelphia PA; 1996:466–490.

[27] Antis G, Chantikul P, Lawn B, Marshall D. A Critical Evaluation of Indentation Techniques for Measuring Fracture Toughness: I, Direct Crack Measurements. J Am Ceram Soc 1981;64:533–8.

[28] Shackelford JF, Alexander W. Material science and engineering handbook, 3rd ed. CRC Press NY; 2001:959.

[29] Hoshii S, Kojima A, Goto M. Preparation of graphitic materials by spark plasma sintering method. J Mater Sci Lett 2001;20:441–3.

[30] Chan M, Seung Ch, Kyung K, Kyung L, Soon H. Fabrication of carbon nanotube reinforced alumina matrix nanocomposite by sol–gel process. Mater Sci Eng A 2005;395:124–8.

Table 1

Samples	Relative density (%)	Fracture strenght (MPa)	Vickers Hardness (Kg/mm^2)
CNFs+10vol.% Al$_2$O$_3$	89.4	60.8 ± 2.3	62.5 ± 1.7
CNFs+20vol.% Al$_2$O$_3$	89.8	59.4 ± 1.9	63.9 ± 1.2
CNFs+30vol.% Al$_2$O$_3$	90.2	60.9 ± 2.2	95.2 ± 2.2
CNFs+40vol.% Al$_2$O$_3$	93.5	63.4 ± 2.6	134.1 ± 2.8
CNFs+50vol.% Al$_2$O$_3$	95.9	134.3 ± 3.2	211.7 ± 2.6

Table 1. Characteristics of CNFs/Al$_2$O$_3$ composites materials obtained from mixing powders and fabricated by SPS at 1500 ºC and 80 MPa for 1 min in a vacuum.

Table 2

Samples	T_i^a	T_2^b	T_f^b	ΔT_1^c	ΔT_2^d	T_{max}^d	wt.%$_1$	wt.%$_2$
Colloidal	160	360	680	200	320	225	12	10
Sol-gel	200	360	680	160	320	285	32	8

a Temperature of initial weight loss (ºC)
b Temperature of final weight loss (ºC)
c Difference between Tf and T_2 (ºC)
d Difference between T_2 and Ti (ºC)
e Temperature of maximum rate of weight loss (ºC)
f Weight loss in ΔT_1
g Weight loss in ΔT_2

Table 2. Thermogravimetric data of the coated CNFs/Al$_2$O$_3$ powders.

Table 3

Samples	Relative density (%)	Fracture strength (MPa)	Vickers hardness (Kg/mm^2)
CNFs+10vol.% Al$_2$O$_3$ (Mixing powders)	89.4	60.8 ± 2.3	62.5 ± 1.7
CNFs+10vol.% Al$_2$O$_3$ (Colloidal)	92.3	65.9 ± 2.8	57.5 ± 1.4
CNFs+10vol.% Al$_2$O$_3$ (Sol-Gel)	93.5	89.5 ± 3.2	60.9 ± 0.9

Table 3. Properties of CNFs+10vol.% Al$_2$O$_3$ composites obtained from mixing powders, colloidal and sol-gel methods and fabricated by SPS at 1500 ℃ and 80 MPa for 1 min in vacuum.

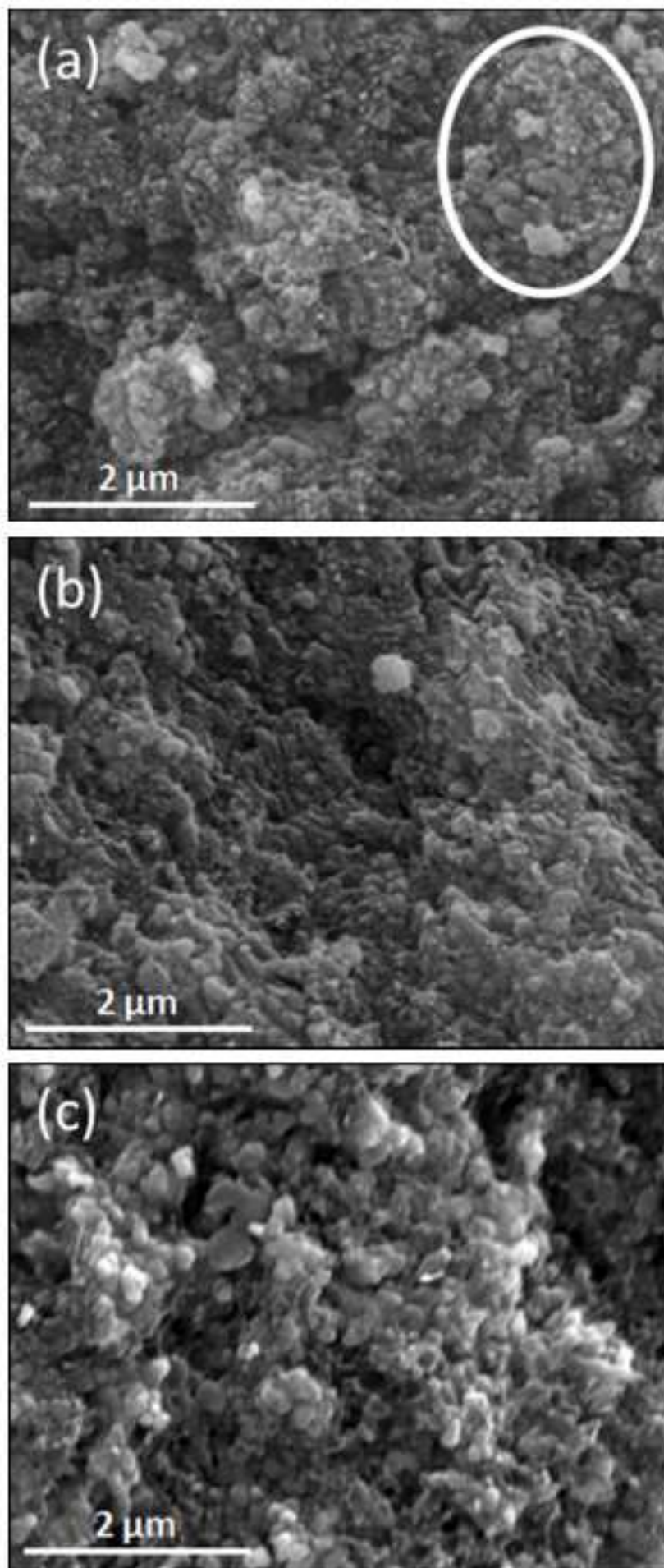**Figure 1**
Click here to download high resolution image

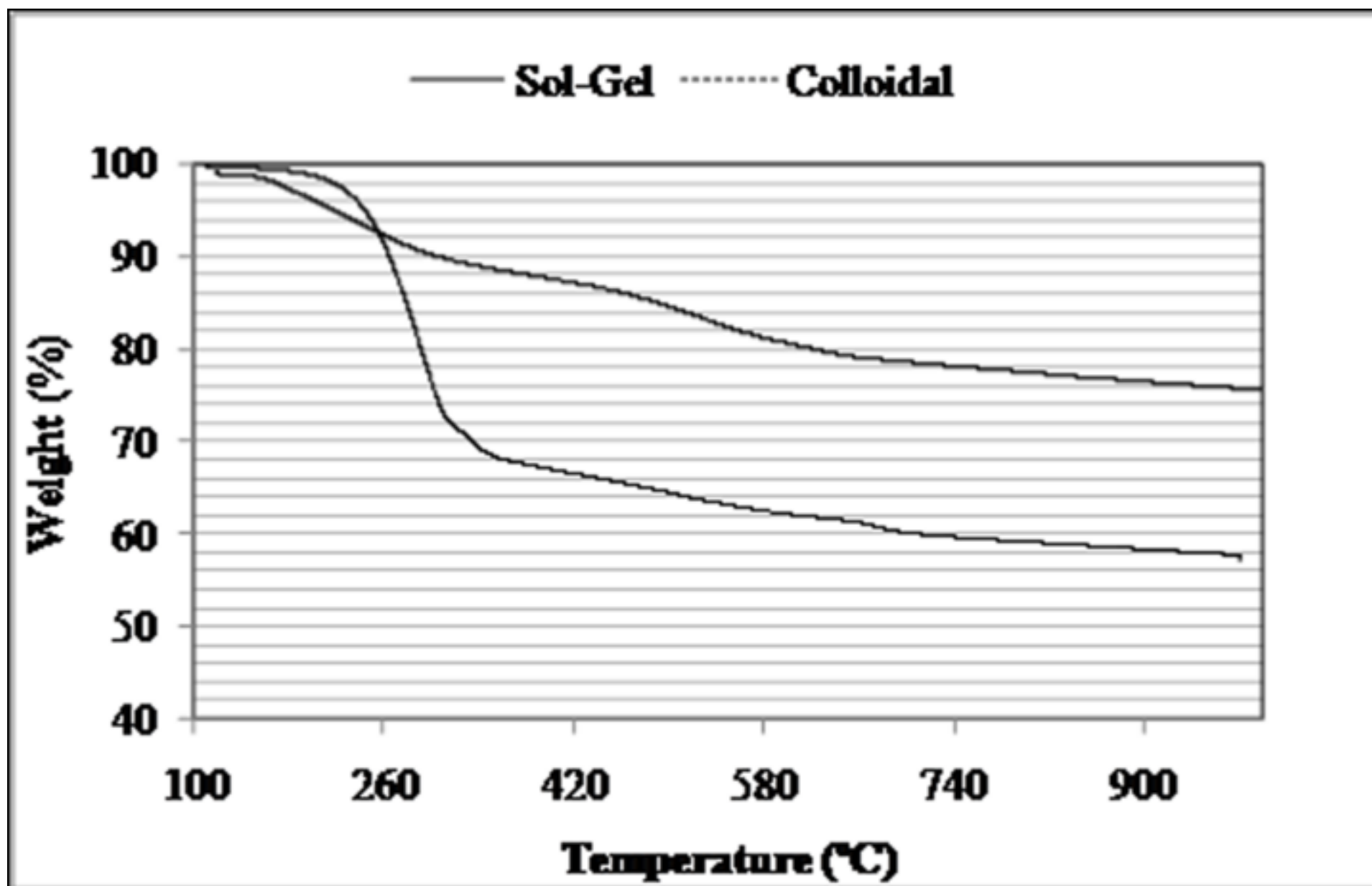**Figure 2**
Click here to download high resolution image

Figure 2

Figure 3
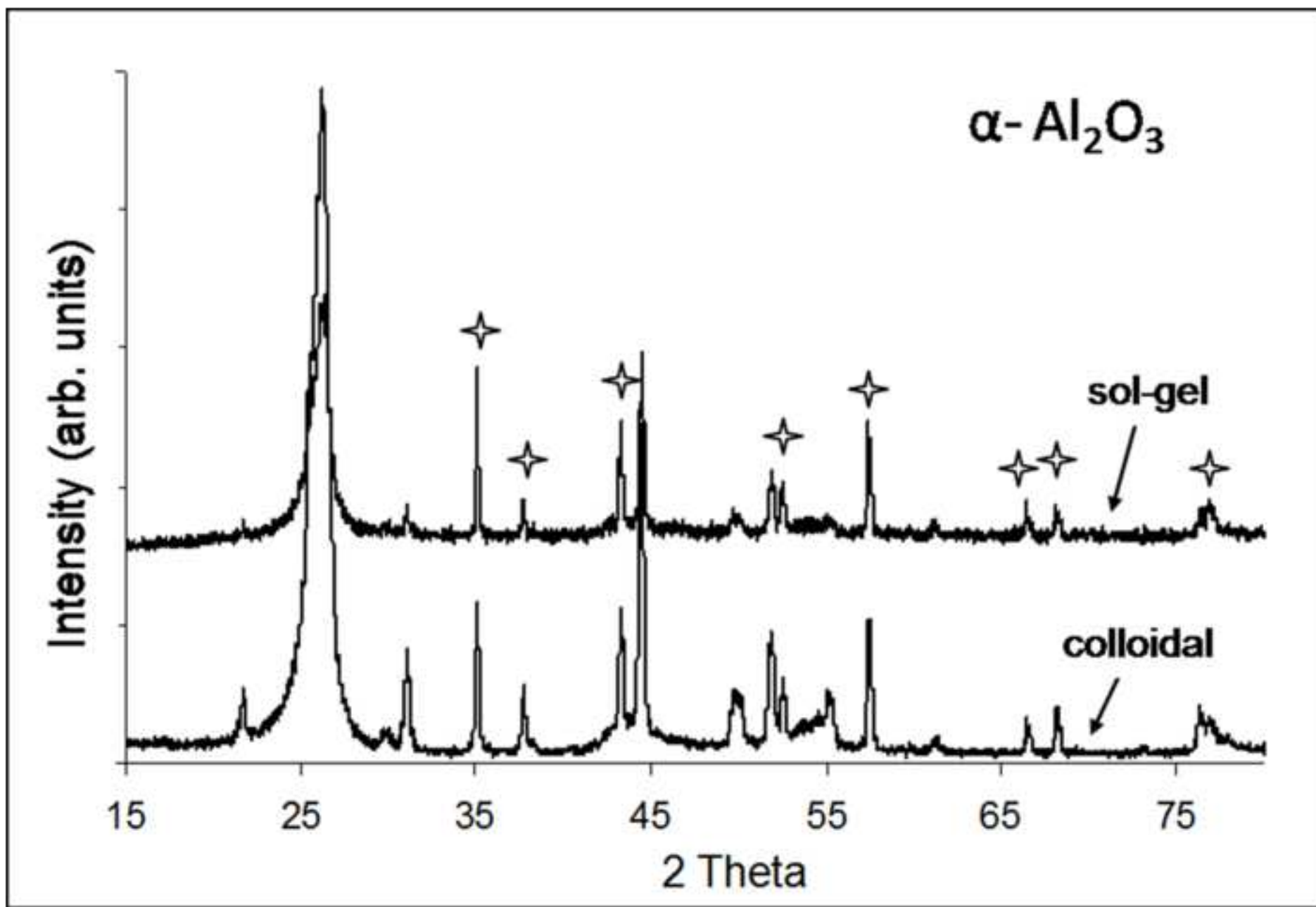**Click here to download high resolution image**

Figure Captions

Figure 1. SEM micrographs of fracture surfaces of the CNFs/Al$_2$O$_3$ sintered materials by SPS at 1500 ℃ with: (a) 10, (b) 40 and (c) 50 vol.% Al$_2$O$_3$.

Figure 2. TG analysis of the powders synthesized by colloidal and sol-gel methods.

Figure 3. XRD patterns of the powders prepared by the colloidal and sol-gel methods and sintered by SPS at 1500 ℃.